

Modeling and control for Vertical Rail Vehicle Dynamic Vibration with Comfort Evaluation

Mortadha Graa

Abstract— Investigation of control vibration is an important topic for the purposes of ride comfort in railway engineering. The vibration of rail vehicles becomes very complex because it is affected by the condition of vehicles, including suspensions and wheel profile, condition of track sections, including rail profile, rail irregularities, cant and curvature. The present study deals with the modeling and control for vertical active suspension rail vehicle by PID-ZN controller. A model of 17 degrees of freedom is adopted which consists of one car body 2 bogies and 4 wheel-sets. A Sperling ride index (ISO2631) is calculated using filtered RMS accelerations in order to evaluate the ride comfort. It should be noticed that the control model was carried out to improve Wz index about 41% at speed of 60 m/s.

Keywords— ISO 2631, active suspension, passive suspension, PID controller, rail vehicle, comfort.

I. INTRODUCTION

Rail comfort is one of the priority axes of the designers of rail vehicles. However, the comfort that passengers experience is usually perceived differently from one individual to another. The nature of vibration itself is random and covers a wide frequency range [1]. The improvement of the passenger comfort while travelling has been the subject of intense interest for many train manufacturers, researchers and companies all over the world. Although new techniques in manufacturing and design ensure better ride quality in railway carriages, it is sometimes impossible to completely eliminate track defects or various ground irregularities.

Several studies have been performed on rail vehicle with passive suspensions. Nejlaoui et al [2] optimized the structural design of passive suspensions in order to ensure simultaneously passenger safety and comfort. Abood et al [3] investigated the Railway carriage simulation model to study the influence of vertical secondary suspension stiffness on ride comfort of railway car body. Zhang et al [4] developed a finite elements optimization technique to find the best parameters of the passive suspension in order to improve the train riding comfort.

The author is with the Laboratoire de Génie Mécanique (LGM) Ecole Nationale d'Ingénieurs de Monastir Université de Monastir, Tunisie

The objective is to reach the best compromise between the ride quality and the suspension deflections.

Other works focused on the study of active suspension systems where a controlled actuator is embedded in the system. Zhou et al [5] developed an active lateral secondary suspension of railway vehicles in order to attenuate the vehicle body lateral vibration. This active suspension is controlled by the use of skyhook dampers. To decrease the effect of road vibration problems, Eski et al [6] controlled the vibration of the vehicle suspension by using a PID controller. The LQR method was also used in designing active suspensions [7, 8].

There exists complex dynamics between the rail and wheel. In fact, an accuracy modeling of the rail vehicle dynamics is often difficult. In the physical system, the input comes from the actual track. In a model, the user-defined input can be created analytically or can be based on actual measurements. For this study analytic track data are created using mathematical shapes, to represent the track geometry [10].

II. DYNAMIC MODELING OF A RAIL VEHICLE

The multi body system is composed from rigid bodies, interconnected via springs, dampers and, eventually, actuators combined in primary and secondary suspensions of railway vehicles.

A. Assumptions

The following general assumptions are considered in developing the proposed model:

- The RV has a longitudinal plane of symmetry (i.e., the centers of gravity of all masses lie in a central plane).
- All springs and dampers are assumed to be linear
- No contact loss between the wheel and the rail.
- The vehicle is moving with constant velocity.
- The irregularity is in the vertical direction with the same shape for left and right rails.

B. Rail vehicle model

A schematic representation of the rail vehicle system is shown in Fig.1. The RV consists of one car body, two bogies and two wheel-sets per bogie (total of four wheel-sets). Each bogie consists of the bogie, and two wheel

sets. The car body is modeled as a rigid body having a mass M_c ; and having moment of inertia J_{cx} and J_{cz} about the longitudinal and transverse axes, respectively. Similarly, each bogie frame is considered as a rigid body with a mass m_b (m_{b1} and m_{b2}) with moment of inertia J_{bx} and J_{by} about the longitudinal and transverse axes, respectively. Each axle along with the wheel set has a mass m_w (for four axles m_{w1} ; m_{w2} ; m_{w3} and m_{w4}). The spring and the shock absorber in the primary suspension for each axle are characterized by spring stiffness K_p and a damping coefficient C_p , respectively. Likewise, the secondary suspension is characterized by spring stiffness K_s and a damping coefficient C_s , respectively. As the vehicle carbody is assumed to be rigid, its motion may be described by the vertical displacement (bounce or z_c) and rotations about the transverse horizontal axis (pitch or ϕ_c) and about the longitudinal horizontal axis (roll or θ_c). Similarly, the movements of the three bogie units are described by three degrees of freedom z_b , ϕ_b and θ_b , each about their centers. Each axle set is described by two degrees of freedom z_w ; and θ_w about their centers. Totally, 17 degrees of freedom have been considered in this study for the vehicle model shown in Fig.1. Table I presented the detailed parameters regarding the moment of inertia and mass of different component.

To minimize the car body vibrations, four vertical actuators are designed: one vertical right and one vertical left controller actuator per bogie in a vehicle, (Fig.1).

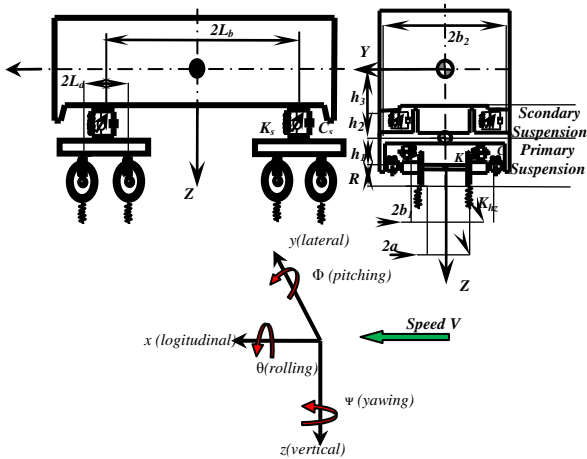


Fig.1. Physical model of railway vehicle

TABLE I. PARAMETERS OF RIGID BODIES

Rigid Bodies	Mass (Kg)	Moment of Inertia (Kg.m ²)	
		J_x	J_z
Car Body	$6,7 \times 10^5$	10^5	10^5
Bogie-I and II	10^5	10^5	10^5
Wheel-set-I,II,III and IV	4000	4000	4000

The vertical controllers are designed to suppress car body vertical, pitch and roll angular vibrations caused by vertical rail disturbances.

Control force vector can be given as: ($i = 1, 2, j = 1..4$)

$$[F_u] = [F_c^u \quad F_{bi}^u \quad F_{wj}^u] \quad (1)$$

Where F_c^u , F_{bi}^u and F_{wj}^u are the car body, bogie i and wheel-set j control forces, respectively, given in following:

$$F_c^u = \begin{bmatrix} \sum_{j=1}^4 u_{zj} \\ b_2 \sum_{i=1}^2 (u_{z(2i)} - u_{z(2i-1)}) \\ L_b [(u_{z3} + u_{z4}) - (u_{z1} + u_{z2})] \end{bmatrix}^T \quad (2)$$

$$F_{bi}^u = [- (u_{z(2i)} + u_{z(2i-1)}) \quad -b_2 (u_{z(2i)} - u_{z(2i-1)}) \quad 0] \quad (3)$$

$$F_{wj}^u = [0 \quad 0 \quad 0] \quad (4)$$

C. Equations of motion

The equations of motion of the railway vehicle are obtained by means of the Lagrange equation. We obtained the following equations of motion for the wheel-set j :

$$m_{wj} \ddot{z}_{wj} + 2C_p [-\dot{z}_{bi} + \dot{z}_{wj} - L_d \dot{\phi}_{bi}] + 2K_p [-z_{bi} + z_{wj} - L_d \phi_{bi}] + K_{hz} [2z_{wj} - (z_{rk} + z_{r(k+1)})] = 0 \quad (5)$$

$$J_{xwj} \ddot{\theta}_{wj} + 2b_1^2 C_p [-\dot{\theta}_{bi} + \dot{\theta}_{wj}] + 2b_1^2 K_p [-\theta_{bi} + \theta_{wj}] + aK_{hz} [2a\theta_{wj} + (z_{rk} + z_{r(k+1)})] + R_1^2 K_{hz} \theta_{wj} = 0 \quad (6)$$

where $j = 1, 2$ when $i = 1$, $j = 3, 4$ when $i = 2$, $k=1$ when $j=1$, $k=3$ when $j=2$, $k=5$ when $j=3$, $k=7$ when $j=4$; the dot indicates differentiation with respect to time variable t .

The equations of motion of the bogie i are:

$$m_{bi} \ddot{z}_{bi} + 2C_p [2\dot{z}_{bi} - (\dot{z}_{wj} + \dot{z}_{w(j+1)})] + 2C_s [-\dot{z}_c + \dot{z}_{bi} + kL_b \dot{\phi}_c] + 2K_p [2z_{bi} - (z_{wj} + z_{w(j+1)})] + 2K_s [-z_c + z_{bi} + kL_b \phi_c] = -u_{zj} - u_{z(j+1)} \quad (7)$$

$$J_{xbi} \ddot{\theta}_{bi} + 4h_1^2 C_p \dot{\theta}_{bi} + 2h_2 C_s [h_3 \dot{\theta}_c + h_2 \dot{\theta}_{bi} + kL_b \dot{\psi}_c] + 4b_1^2 C_p \dot{\theta}_{bi} + 2b_2^2 C_s [-\dot{\theta}_{bi} + \dot{\theta}_c] + 4h_1^2 K_p \theta_{bi} + 2h_2 K_s [h_3 \theta_c + h_2 \theta_{bi}] + 4b_1^2 K_p \theta_{bi} + 2b_2^2 K_s [\theta_{bi} - \theta_c] = -b_2 (u_{z(j+1)} - u_{zj}) \quad (8)$$

$$J_{ybi} \ddot{\phi}_{bi} + 2L_d C_p [2L_d \dot{\phi}_{bi} + (\dot{z}_{wj} - \dot{z}_{w(j+1)})] + 2L_d K_p [2L_d \phi_{bi} + (z_{wj} - z_{w(j+1)})] = 0 \quad (9)$$

where $j = 1$ and $k=1$ when $i = 1$; $j = 3$ when $i = 2$; $j=5$ and $k=1$ when $i=3$.

Finally, the equations of motion of the car body are:

$$m_c \ddot{z}_c + 2C_s \left[3\dot{z}_c - \sum_{p=1}^2 \dot{z}_{bp} \right] + 2K_s \left[3z_c - \sum_{p=1}^2 z_{bp} \right] = \sum_{p=1}^4 u_{zp} \quad (10)$$

$$J_{xc} \ddot{\theta}_c + 2h_3 C_s \left[3h_3 \dot{\theta}_c + h_2 \sum_{p=1}^2 \dot{\theta}_{bp} \right] + 2b_2^2 C_s \left[3\dot{\theta}_c - \sum_{p=1}^2 \dot{\theta}_{bp} \right] + 2h_3 K_s \left[3h_3 \theta_c + h_2 \sum_{p=1}^2 \theta_{bp} \right] + 2b_2^2 K_s \left[3\theta_c - \sum_{p=1}^2 \theta_{bp} \right] = b_2 \left[\sum_{p=1}^2 u_{z2p} - \sum_{p=0}^1 u_{z(2p+1)} \right] \quad (11)$$

$$J_{yc} \ddot{\phi}_c + 2L_b C_s [2L_b \dot{\phi}_c + (\dot{z}_{b1} - \dot{z}_{b3})] + 2L_d K_s [2L_b \phi_c + (z_{b1} - z_{b3})] = L_b [(u_{z3} + u_{z4}) - (u_{z1} + u_{z2})] \quad (12)$$

III. TRACK INPUTS TO RAIL ROAD VEHICLE

In actual practice periodic, a-periodic or random track irregularities may exist on the track, but in the present study bump type of irregularity is considered as shown in Fig.2 [10].

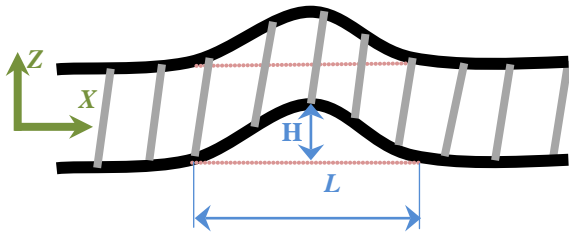


Fig.2. Model of track irregularity

The bump excitations of the left wheels (Fig.3) of leading bogies are as follows:

$$Z_{ri} = \begin{cases} \frac{H}{2} \left[1 - \cos \left(2\pi \frac{V}{L} (t - t_{di}) \right) \right] & \text{for } t_{di} \leq t \leq \frac{L}{V} + t_{di} \\ 0 & \text{otherwise} \end{cases} \quad (13)$$

$(i = 1..4)$

Where $[t_{d1}, t_{d2}, t_{d3}, t_{d4}] = \left[0, \frac{2L_d}{V}, \frac{2L_b}{V}, \frac{2L_b + 2L_d}{V} \right]$ (14)

For this study, H and L are taken as, respectively, $0.03m$ and $1m$.

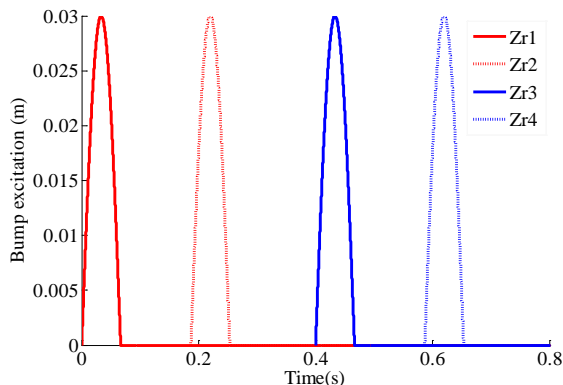


Fig.3. The bump excitations of the left wheels vehicle speed of 30 m/s

IV. CONTROL STRATEGIES AND DESIGN

In this section, the design of the PID controller for improving the ride passenger comfort is presented.

The different controller gains will be determined according to the rail vehicle dynamic. The PID controller block diagram is given in Fig.4. The objective of the PID is to minimize an error $e(t)$ through the control of the active suspension. The output of the PID controller is given by:

$$u_{zi}(t) = K_p e(t) + K_i \int_0^t e(s) ds + K_D \frac{de(t)}{dt} \quad (15)$$

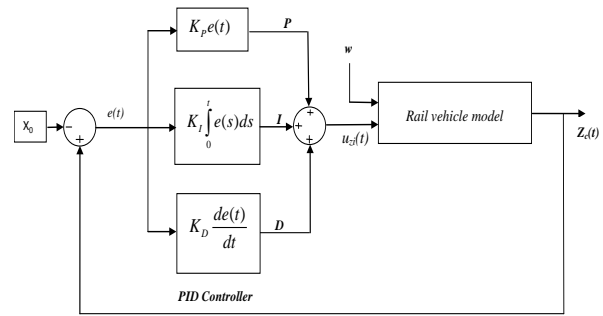


Fig.4. The block diagram of PID controller

Where K_p, K_i and K_D are proportional, integral and derivative gains, respectively. $u_{zi}(t)$ is the control force.

We will substitute the PID controller and the open loop return with a level step. To find the values of the PID gains, we have used the step response Ziegler-Nichols method [11, 12]. TABLE II presents these gains.

Vertical control force	K_p	K_D	K_i
$u_{zi}(i=1..4)$	187	25401	43535

V. SPERLING RIDE INDEX

We can define Sperling's ride index as [13, 14, 15, 16]:

$$W_Z = \left(\sum_{i=1}^{n_f} W_{Zi}^{10} \right)^{\frac{1}{10}} \quad (16)$$

Where n_f is the total number of discrete frequencies of the acceleration response of the railway vehicle identified by the FFT and W_{Zi} is the comfort index corresponding to the i th discrete frequency, given by:

$$W_Z = \left[a_i^2 B(f_i)^2 \right]^{\frac{1}{6.67}} \quad (17)$$

Where a_i denotes the amplitude of the peak acceleration response (in cm/s^2) measured on the floor of the itch frequency identified by the FFT and $B(f_i)$ a weighting factor, given by:

$$B(f) = k \sqrt{\frac{1.911f^2 + (0.25f^2)^2}{(1 - 0.277f^2)^2 + (1.563f - 0.0368f^3)^2}} \quad (18)$$

Where $k = 0.737$ for horizontal vibration and 0.588 for vertical vibration.

VI. RESULTS DISCUSSION AND COMFORT IMPROVEMENT

A. Rail vehicle design parameters

The used design parameters of rail vehicle are presented in Table III. The models were built in the MATLAB/Simulink® environment. The fixed step solver ODE-45 (Dormand-Prince) was utilized, with the sampling time $T_s=0.001s$. T_s is smaller than the fastest half-car Active Vehicle Suspension Systems (AVSS) model dynamics, enabling observation of all model dynamic[17, 18]. Dynamic behavior analysis for the different compounds

of the rail vehicle system was carried out for the vehicle at different speeds: 30 m/s, 45 m/s and 60 m/s.

TABLE III. RAIL VEHICULE DESIGN PARAMETERS

Nomenclature	Values
K_p	$10^6 N/m$
K_s	$1,7 \times 10^9 N/m$
C_p	$6 \times 10^4 Ns/m$
C_s	$10^5 Ns/m$
K_{hz}	$35 \times 10^9 N/m$
L_b	6 m
L_d	1,4 m
d_p	1 m
d_s	1 m
a	0,7163 m
b_1	1 m
b_2	1 m
R_1	0,61 m
h_1	0,3 m
h_2	0,2 m
h_3	1,3 m

The displacement and acceleration responses of the car body at speeds of 30m/s, 45m/s, 60m/s are shown, respectively, in Fig.5 and Fig.6. Plots show that initially, the value of acceleration is nearly equal to 0 m/s², which is mainly the acceleration without gravity. The following output parameters are evaluated:

- Vertical displacement and acceleration at the floor of the car body center of mass in time and frequency domain.
- Vertical acceleration at the front and the rear bogie center of mass in time domain.

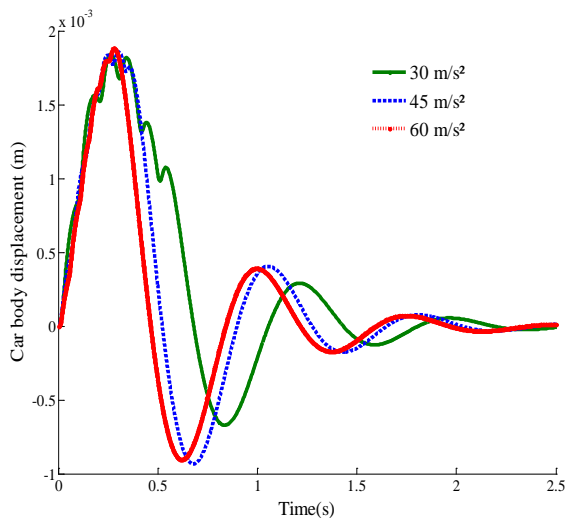


Fig.5. The vertical car body displacement for different vehicle speeds. The vibration of the car body ceases and stabilizes. The displacement and acceleration are generally within an acceptable range and does not show any instability.

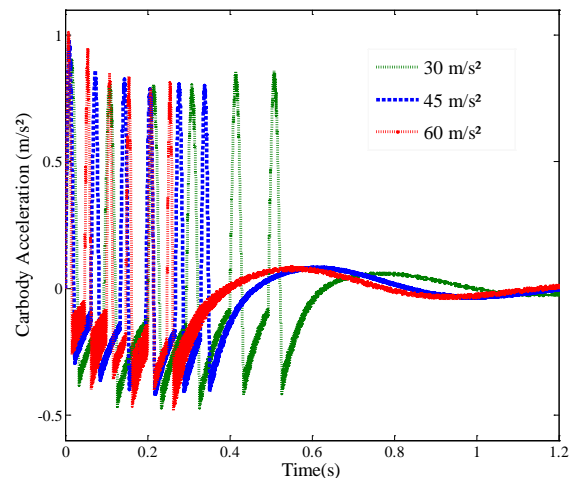


Fig.6. The vertical car body displacement for different vehicle speeds. Fig.7 and Fig.8, respectively, shows the acceleration response of front and the rear bogie with time at different speeds.

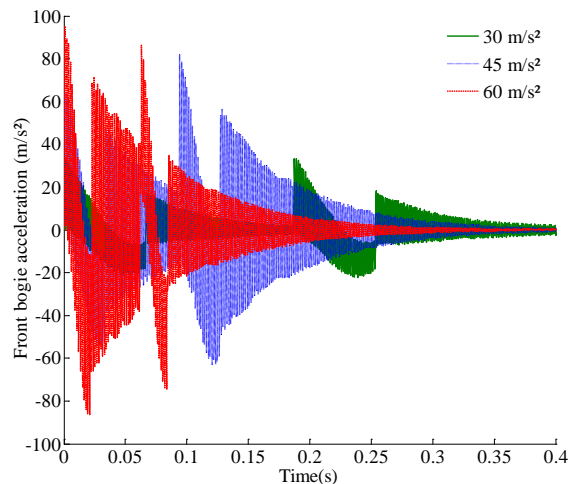


Fig.7. The vertical front bogie acceleration for different vehicle speeds

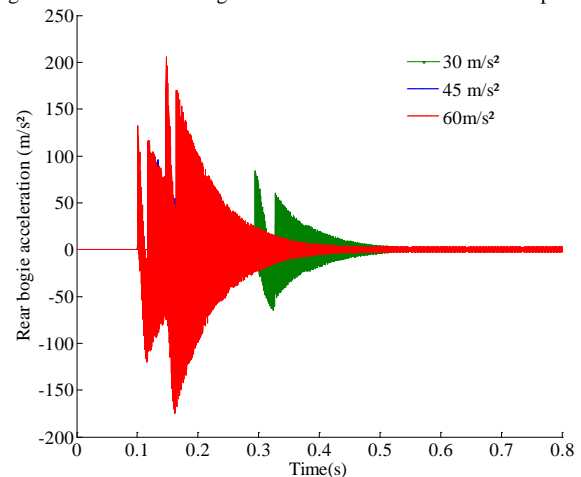


Fig.8. The vertical rear bogie acceleration for different vehicle speeds

We can note that the amplitude of the vehicle vibration increased with the vehicle speed. It is also clear from the plots that initially the wheels of the front bogies come in contact with the track irregularity and the vibration starts in the front bogie and later these vibrations are shifted to the rear bogies.

B. Comfort evaluation

Fig.9 and Fig.10 presents, respectively, the vertical car body displacement and the vertical car body acceleration at the speed of 60 m/s.

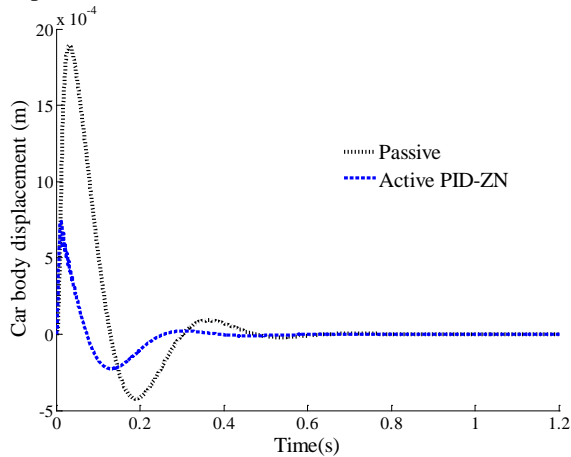


Fig.9.The vertical car body displacement for 60 m/s

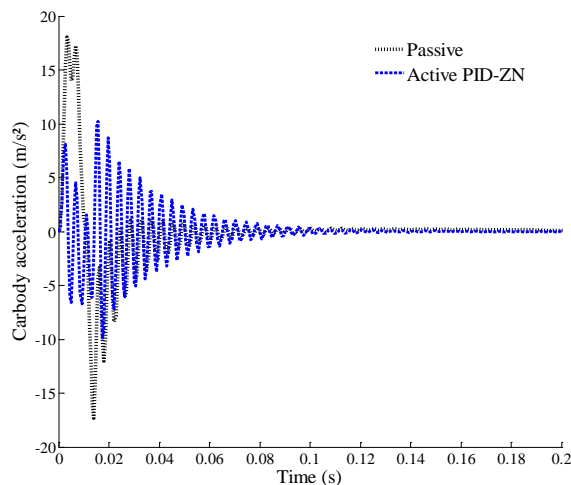


Fig.10.The vertical car body acceleration for 60 m/s

It can be observed that, in the case of the active PID-ZN controller, the reduction of the car body’s vertical displacement peak is approximately 63% and the reduction of the car body’s vertical acceleration peak is approximately 55% compared to passive suspension. Acceleration frequency response plots were generated for car body at vehicle speeds of 30 m/s to 60 m/s and are shown in figure.11 to calculate the Sperling ride comfort index. The FFT plot is generated for a frequency range between 0 to 25 Hz, as the human beings are most sensitive in the frequency range of 4 to 12.5 Hz. Ride comfort analysis has been performed for speeds ranging from 30m/s to 60m/s.

The analysis has been performed on the system model to calculate the vertical acceleration of the system. FFT output is taken to get the peak acceleration frequency component. Comfort index has been calculated through Eqs [16-18], which are presented in Table IV.

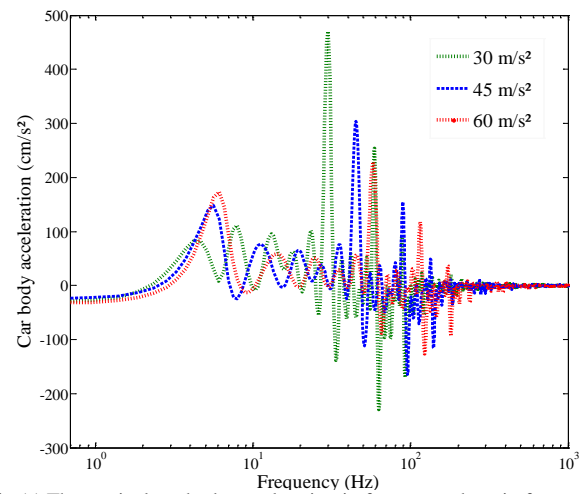


Fig.11.The vertical car body acceleration in frequency domain for different speeds

The maximum and minimum ISO Sperling Index values are respectively 2.53 and 1.62 for the rail vehicle speed respectively 15 m/s and 60 m/s. These values respectively indicate “The more pronounced but not unpleasant” and “just noticeable” zones.

TABLE IV. COMFORT INDEX EVALUATION (PASSIVE SYSTEM)

Vehicle Speed (m/s)	Sperling Index (W_z)	Evaluation
15	2.53	More pronounced but not unpleasant
30	2.03	Clearly noticeable
45	1.72	Just noticeable
60	1.62	Just noticeable

TABLE V. SPERLING’S RIDE COMFORT INDEX (ACTIVE SYSTEM)

Vehicle Speed (m/s)	Sperling Index (W_z)	Evaluation
15	1.64	Just noticeable
30	1.25	Just noticeable
45	1.03	Just noticeable
60	0.95	Just noticeable

The maximum and minimum ISO Sperling Index values are respectively 2.53 and 1.62 for the rail vehicle speed respectively 15 m/s and 60 m/s in passive one. These values respectively indicate “The more pronounced but not unpleasant” and “just noticeable” zones. Fig.12 shows that the comfort index decreases as the vehicle speed increases while maintaining an acceptable level of comfort.

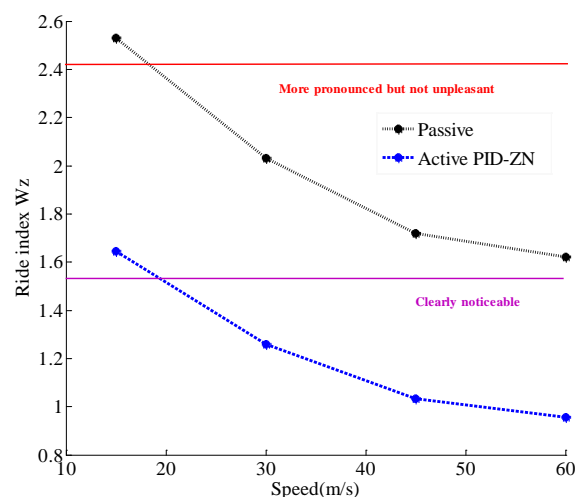


Fig.12.The Sperling index comfort variation for different speeds

This means that the passengers are not much affected by the vibration as they are exposed to low level of vibrations. According to the Table V, the controlled suspension system keeps a low Sperling Index values compared to the passive suspension system (not exceed 1.64). The active PID-ZN controller keeps the passenger in a “just noticeable” level of comfort for all speed values. According to the Table VI, the Sperling’s index improvement increase with rail vehicle speed until 41.35% at speed of 60 m/s.

TABLE VI. IMPROVEMENT OF SPERLING’S RIDE COMFORT INDEX

Vehicle Speed (m/s)	Sperling Index (W_z)	Sperling Index (W_z)	Improvement (%)
15	2.53	1.64	28.06
30	2.03	1.25	38.42
45	1.72	1.03	40.11
60	1.62	0.95	41.35

VII. CONCLUSION

A 17 degree of freedom Railway Vehicle model is developed and used for the vertical control dynamic analysis. A similar irregularity at both right and left rail is considered at same velocity input in all wheel-sets. To calculate Sperling ride index for the above vehicle, a vertical acceleration response at the car body has been calculated in the frequency domain. The Sperling ride Index values at different speeds are presented. The calculated values of the Sperling index are found well in the satisfactory limits defined by the ISO 2631 standard which means that the passengers are not much affected by the vibration as they are exposed to low level of vibrations. It should be noticed that the control model was carried out to improve W_z index about 41% at speed of 60 m/s.

REFERENCES

- [1] D. Skarlatos et al., “Railway fault diagnosis using a fuzzy logic method,” *Applied Acoustic*, vol 65, 951–966, 2004.
- [2] M.Nejlaoui, A. Houidi, Z. Affi, and L. Romdhane, “Multiobjective robust design optimization of rail vehicle moving in short radius curved tracks based on the safety and comfort criteria,” *Simulation Modeling Practice and Theory*, vol 30, 21–34, 2013.
- [3] K. H. A. Abood and R. A. Khan, “The Railway carriage simulation model to study the influence of vertical secondary suspension stiffness on ride comfort of railway carbody,” *Journal of Mechanical Engineering Science*, vol 225, 1349-1359, 2011.
- [4] Y.W. Zhang, Y. Zhao, Y.H. Zhang, J.H. Lin, and X.W. He, “Riding comfort optimization of railway trains based on pseudo-excitation method and symplectic method,” *Journal of Sound and Vibration*, vol 332, 5255–5270, 2013.
- [5] R. Zhou, A. Zolotas and R. Goodall, “9 DOF railway vehicle modeling and control for the integrated tilting bolster with active lateral secondary suspension,” *IEEE, UKACC International Conference on Systems Technology Control*, vol 465, 1-6, 2010.
- [6] I. Eski and S. Yildirim, “Vibration control of vehicle active suspension system using a new robust neural network control system,” *Simulation Modeling Practice and Theory*, vol 17, 778–793, 2009.
- [7] Pratt I, “Active Suspension Applied to Railway Trains,” PhD Thesis, Department of Electronic and Electrical Engineering, Loughborough University, 2002.
- [8] Vincent. J, “ Etude du concept de suspensions actives- Applications aux voitures ferroviaires, ” PhD Thesis, INSA de Lyon, France, 1999.
- [9] H. Kumar, Sujata, “ Vertical dynamic analysis of a typical indian rail road vehicle,” *Proceedings on computational mechanics and simulation*, IIT, India, 8–10, 2006.
- [10] V. Dukkipati, J. Amyot, “Computer Aided Simulation in Railway Dynamics,”. Marcel Dekker, New York, 1988.
- [11] K.H. Ang, G.C.Y. Chong, and Y. Li, “ PID control system analysis, design, and technology,” *IEEE Transactions on Control Systems Technology*, vol 13, 559-576, 2005.
- [12] A. Wolfgang, “ Practical Control for Engineers and Technicians,” 115-117.
- [13] J. Forstberg, “ Ride comfort and motion sickness in tilting trains - Human responses to motion environments in train and simulator experiments,” Master’s Thesis, KTH/ FKT/D-00/28-SE, Division of Railway Technology, KTH, 2000.
- [14] Carg, V. K, “ Dynamics of Railway Vehicule Systems,” Academ Press, NW, 1984.
- [15] B153/RP21 Application of ISO Standard to Railway Vehicules(1993): Comfort Index N_{mv} Comparaison with the ISO/SNCF Comfort Note and with the W_z (European Rail Research Istitute).
- [16] Vivec Kumar and Vikas Rastogi, “ Investigation of vertical dynamic behaviour of a typical indian rail road vehicle bond graph,” *World Journal of Modeling and Simulation*, vol 5, 130-138, 2009.
- [17] Chen.H et al, “ Application of Constrained H_∞ Control to Active Suspension Systems on Half-Car Models,” *Journal of Dynamic Systems, Measurement and Control*, *Transactions of the ASME* vol 127 345-354, 2005.
- [18] Pedro.J. and Dahunsi, O, “Neural Network-based Feedback Linearization Control of a Servo-Hydraulic Vehicle Suspension System,” *International Journal of Applied Mathematics and Computer Science* vol 21, 137-147, 2011.